FRONTIERS OF PHYSICS

RESEARCH ARTICLE
Volume 19 / Issue 2 / 23201 / 2024

Detecting bulk and edge exceptional points in non-Hermitian systems through generalized Petermann factors

Yue-Yu Zou*, Yao Zhou*, Li-Mei Chen*, Peng Ye†

School of Physics, State Key Laboratory of Optoelectronic Materials and Technologies, and Guangdong Provincial Key Laboratory of Magnetoelectric Physics and Devices, Sun Yat-sen University, Guangzhou 510275, China
*These authors contributed equally to this work.
Corresponding author. E-mail: †yepeng5@mail.sysu.edu.cn
Received April 20, 2023; accepted August 14, 2023

ABSTRACT

Non-orthogonality in non-Hermitian quantum systems gives rise to tremendous exotic quantum phenomena, which can be fundamentally traced back to non-unitarity. In this paper, we introduce an interesting quantity (denoted as η) as a new variant of the Petermann factor to directly and efficiently measure non-unitarity and the associated non-Hermitian physics. By tuning the model parameters of underlying non-Hermitian systems, we find that the discontinuity of both η and its first-order derivative (denoted as $\partial\eta$) pronouncedly captures rich physics that is fundamentally caused by non-unitarity. More concretely, in the 1D non-Hermitian topological systems, two mutually orthogonal edge states that are respectively localized on two boundaries become non-orthogonal in the vicinity of discontinuity of η as a function of the model parameter, which is dubbed "edge state transition". Through theoretical analysis, we identify that the appearance of edge state transition indicates the existence of exceptional points (EPs) in topological edge states. Regarding the discontinuity of $\partial\eta$, we investigate a two-level non-Hermitian model and establish a connection between the points of discontinuity of $\partial\eta$ and EPs of bulk states. By studying this connection in more general lattice models, we find that some models have discontinuity of $\partial\eta$, implying the existence of EPs in bulk states.

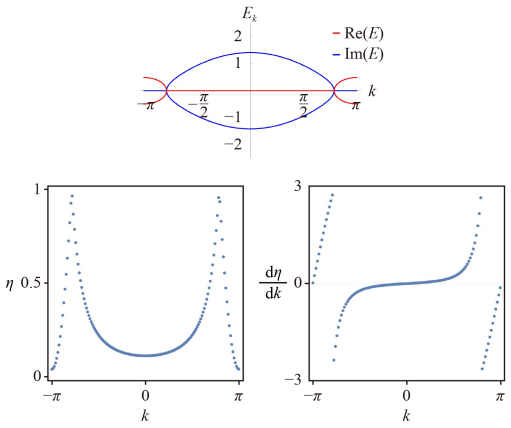

Keywords non-Hermitian, Su–Schrieffer–Heeger (SSH) model, exceptional point

1 Introduction

Recently, non-Hermitian systems [1–6] have drawn great interest, due to exotic quantum phenomena, e.g., generalized bulk-edge correspondence [7–9], exceptional points (EPs) [5, 10–18], non-Hermitian skin effect [7, 19–23] and unidirectional invisibility [24]. To gain a theoretical understanding of these phenomena, non-Bloch band theory [7–9, 25–30], which generalizes the conception of Brillouin zone, is established and applied to analyze the topological phase [5, 31] in non-Hermitian systems. Remarkably, non-Hermitian skin effect, the natural consequence of generalized Brillouin zone, is found to have a connection to EPs [23]. Meanwhile, compared with Hermitian systems, the classification [32–37] of topological phases in non-Hermitian systems has been significantly enriched. In addition, from the quantum-informative perspective, quantum entanglement properties of non-Hermitian systems [38–42] display highly unusual features in entanglement entropy and entanglement spectrum. Besides the crystalline system mentioned before, non-Hermiticity has also been introduced to

Higher Education Press

arXiv: 2208.14944
https://doi.org/10.1007/s11467-023-1337-8

noncrystalline systems, e.g. quasi-crystal systems [42–46] and disorder systems [47–50].

Complex energy spectrum and non-orthogonality are special signs of non-Hermitian physics. While complex energy spectrum is commonly observed in many non-Hermitian systems, real energy spectrum generally holds in systems with $\mathcal{PT}$ symmetry [1, 51]. In our prior work [42], a non-Hermitian quasi-crystal model always has complex energy spectrum which can not be used to characterize its phase transition. Thus, in some non-Hermitian systems, the non-orthogonal eigenstates should be investigated thoroughly for presenting more effective information of non-Hermitian physics. In this paper, to explore physics of non-Hermitian systems, we focus on the property of non-unitarity, i.e., the non-orthogonal eigenvectors [52] which induce interesting phenomena in various research areas [53–60]. When eigenvectors are not mutually orthogonal, the familiar inner product in Hermitian systems is no longer valid and the usual definition of quantum expectation of operators is no longer proper. To proceed further, in the literature, the idea of bi-orthogonal basis is introduced. More concretely, for a non-Hermitian Hamiltonian H, the right eigenvectors $|R,n\rangle$ obey $H|R,n\rangle = E_n|R,n\rangle$, and left eigenvectors $|L,n\rangle$ obey $H^\dagger|L,n\rangle = E_n^*|L,n\rangle$, then bi-orthogonality relation can be represented as $\langle L,n|R,m\rangle = \delta_{nm}$. When the system remains unitarity, $\langle L,n|L,m\rangle = \langle R,n|R,m\rangle = \delta_{nm}$. Thanks to the bi-orthogonality relation, many theoretical approaches originally introduced in Hermitian systems can be borrowed to study non-Hermitian systems. Therefore, a series of physical conceptions are reproduced in non-Hermitian systems [19, 25, 31, 61].

By using bi-orthogonal basis, we can study non-Hermitian quantum systems by constructing Hilbert space. However, it is still unclear how to simply and efficiently characterize non-unitarity arising from the non-orthogonality among right-eigenvectors (or left-eigenvectors). To discuss non-unitarity of non-Hermitian systems, without loss of generality, we focus on studying the property of right basis but not the whole bi-orthogonal basis in this work (because left eigenvectors have the similar property with right eigenvectors). In this paper, generalizing the idea of Lee–Wolfenstein bound [52, 62] for all eigenstates of a non-Hermitian system, we define a quantity to measure the strength of non-unitarity of non-Hermitian systems as follows:

$$\eta = \frac{\sum_{n<m} |\langle R,n|R,m\rangle|^2}{\sum_{n<m} |\langle R,n|R,n\rangle||\langle R,m|R,m\rangle|}, \tag{1}$$

where $0 \le \eta \le 1$. When $\eta = 0$, the system is unitary with mutually orthogonal eigenvectors. On the contrary, when $\eta = 1$, the eigenvectors are totally coalescent, resulting in the extreme case of non-unitarity. Additionally, the definition of the quantity η can be considered as a new variant of the Petermann factor which has various definitions as given in Refs. [4, 53, 63].

Table 1 The correspondence between the location of EPs and the discontinuity of η and its derivative $\partial\eta$ in the models I–IV.

Discontinuity	EPs	Model
η	Topological edge states	I
$\partial\eta$	Bulk states	II, III, IV

In this paper, we study the behavior of the quantity η in various interesting non-Hermitian models as the system parameters varying. We observe the various behaviors of the quantity η, such as the discontinuity of the quantity η and its first-order derivative $\partial\eta$, which imply respectively the existence of EPs in topological edge and bulk states of non-Hermitian systems, as illustrated in Table 1. Specifically, when a non-Hermitian topological system undergoes an *edge state transition* in thermodynamic limit, where the orthogonal edge states become non-orthogonal, the quantity η would have discontinuity point which implies EPs appearing in the topological edge states. For studying the physical consequence causing the discontinuity of $\partial\eta$, we utilize a two-level model exhibiting that when the quantity η near the EP of bulk states, $\partial\eta$ would become discontinuous. Thus, this feature of η can be considered evidence for identifying the existence of EPs in bulk states. Furthermore, using this feature, we infer that the bulk states of some non-Hermitian lattice systems possess EPs.

2 Edge state transition and edge EPs at the discontinuity of η

To focus on non-unitarity of non-Hermitian systems, we consider the behavior of the quantity η in a 1D non-reciprocal Su–Schrieffer–Heeger (SSH) model [64]:

$$\textbf{Model-I}\ H = \sum_n [t_1 c_{n,A}^\dagger c_{n,B} + t_1 c_{n,B}^\dagger c_{n,A} + (t_2+g) c_{n,B}^\dagger c_{n+1,A} + (t_2-g) c_{n+1,A}^\dagger c_{n,B}], \tag{2}$$

where $c_{n,A}$ ($c_{n,B}$) respectively denote annihilation operators of spinless fermions at sublattice A (B) in the nth unit cell. We restrict the parameters g, $t_{1,2}$ in the real regime. When the parameters satisfy the condition $|t_1| < \sqrt{t_2^2 - g^2}$, the system is in a non-Hermitian topological phase with non-trivial winding number and two topological edge states. When $|t_1| > \sqrt{t_2^2 - g^2}$, the system is in a trivial phase without topological edge states. Thus, a topological phase transition occurs at $|t_1| = \sqrt{t_2^2 - g^2}$, which can be identified by the appearance/disappearance of zero energy modes in Fig. 1(a). Meanwhile, we study the quantity η as a function of t_1 in the model-I (2). We find that the phase transition point coincides with the local maximum of η in Fig. 1(b), while the derivative $\partial\eta$ in

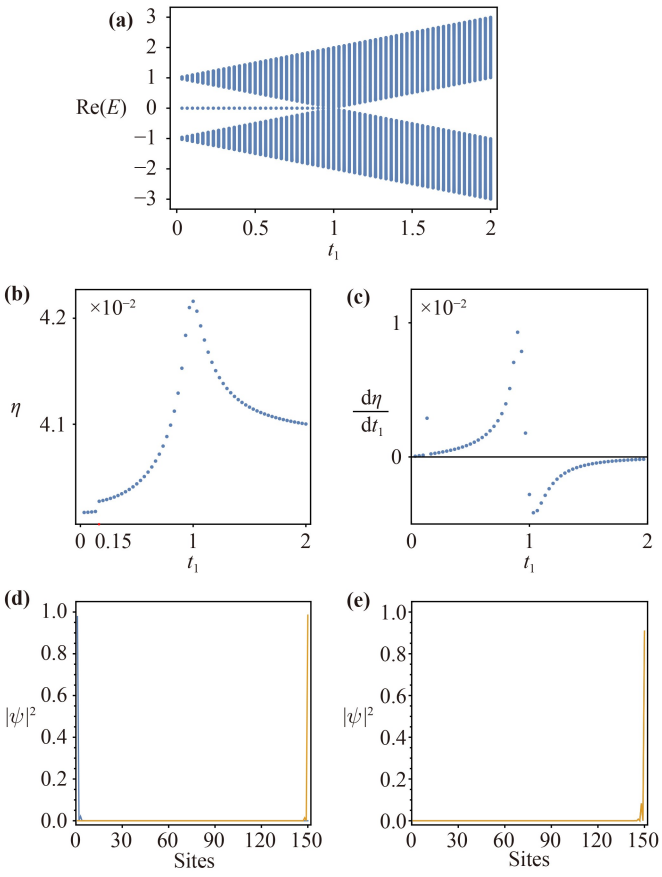

Fig. 1 **(a)** Real part of energy spectrum of the model-I (2) as a function of t_1. The topological phase transition occurs at $t_1 = \sqrt{t_2^2 - g^2} \approx 0.99$. **(b)** and **(c)** respectively show the quantity η and its derivative as a function of t_1. The discontinuity of η and the local maximum of η appear respectively at $t_1 \approx 0.15$ and $t_1 \approx 0.99$. **(d)** and **(e)** respectively demonstrate two distributions of edge states at $t_1 = 0.133$ and $t_1 = 0.333$ near the discontinuity point $t_1 = 0.15$ of the quantity η. Here, $t_2 = 1, g = 0.1$, the length of the system (2) $L = 150$.

Fig. 1(c) is continuous at the transition point. Based on the method of generalized Brillouin zone in Refs. [7–9], we analytically obtain the effective bulk Hamiltonian of the model-I (2) with open boundary condition (more detailed derivation see Appendix A). By using the effective bulk Hamiltonian, when $t_2 = 1$ and $g = 0.1$, the bulk states at topological transition point of the model-I (2) do not have EPs.

Furthermore, we numerically realize that this model exhibits a significant discontinuity of η at $t_1 = 0.15$ with ignoring finite-size effect in Fig. 1(b). To clarify the physical nature of the discontinuity of η, we plot the edge states of the system of two parameter points $t_1 = 0.133$ and $t_1 = 0.333$ near the discontinuity point $t_1 = 0.15$ in Figs. 1(d) and (e), respectively. We find that the topological edge states separately localized at two boundaries are orthogonal in Fig. 1(d), while in Fig. 1(e), the two edge states are simultaneously localized at one boundary and become non-orthogonal. These phenomena are found in recent Refs. [64–67], and we propose that the discontinuity of η appearing in thermodynamic limit can be connected with these phenomena.

Next, we analytically obtain the topological edge states of the model-I (2) in topological phase to explain the appearance of discontinuity points of η in thermodynamic limit. As discussed in Appendix B, when consider the thermodynamic limit ($N \to \infty$), the two zero-energy edge states are expressed as $\phi_{n,A} = (-\frac{t_1}{t_2 - g})^{n-1}\phi_{1,A}$ and $\phi_{1,B} = (-\frac{t_1}{t_2 + g})^{n-1}\phi_{n,B}$, where $\phi_{n,A(B)}$ is the wavefunction on the sublattice $A(B)$ in the nth unit cell. From the expression of $\phi_{n,A(B)}$, we can determine the localization behaviors of the edge states. Furthermore, to satisfy the boundary conditions $\phi_{1,B} = \phi_{N,A} = 0$ (here set $t_2 = 1, g = 0.1$), when $t_1 < t_2 - g$, the wavefunctions $\phi_{n,A}$ and $\phi_{n,B}$ are respectively localized at the left and right endpoints of the 1D chain, and have no contribution to η. When $t_1 > t_2 - g$, to satisfy the boundary condition, we find the wavefunction $\phi_{n,A}$ should satisfy the relation $\phi_{n,A} = \phi_{N,A} = 0$. Then, the wavefunction $\phi_{n,A}$ disappears. For this reason, we can consider the two topological edge states merge into one topological edge state and are simultaneously localized at the right endpoint of the 1D chain and have contribution to η. Therefore, based on above discussion, we propose that the model-I (2) has edge state transition which causes the discontinuity of η with the parameter t_1 varying and satisfy our numerical results in Figs. 1(d) and (e). Furthermore, based on Ref. [66], we find that the edge state transition of this model-I (2) is induced by EPs in topological edge states, where the EPs are called edge EPs. Moreover, it should be noted that the numerical precision of diagonalizing the Hamiltonian matrix of the model-I (2) would influence the location of discontinuity points of η, where this phenomenon originates from the finite-size effect.

3 Bulk EP at the discontinuity of $\partial\eta$

In the following, we move to the physics of discontinuity of $\partial\eta$, i.e., the first order derivative of η. For the purpose, as a warm-up, we introduce a two-level system to study the behavior of the quantity η:

$$\textbf{Model-II}\quad H_0 = \begin{pmatrix} 0 & \gamma \\ 1 & 0 \end{pmatrix}, \tag{3}$$

where $\gamma \in \mathbb{R}$. By diagonalization, the (right-)eigenvectors of H_0 can be obtained and written as $(\pm\sqrt{\gamma}, 1)^{\mathrm{T}}$, which results in an analytic form of $\eta = \frac{|1-|\gamma||^2}{(1+|\gamma|)^2}$. It is apparent that when $\gamma = 1$, the model H_0 becomes Hermitian with $\eta = 0$. On the contrary, when $\gamma = 0$, H_0 reduces to a lower triangular matrix which describes a typical EP, and the quantity $\eta = 1$. Next, we study the behavior of the quantity η as a function of γ near the EP. When $\lambda = \pm\delta$ and $\delta \to 0^+$, the quantity $\eta|_{\lambda=\delta^\pm} = \frac{(1\mp\delta)^2}{(1\pm\delta)^2}|_{\delta\to 0^+} = 1$,

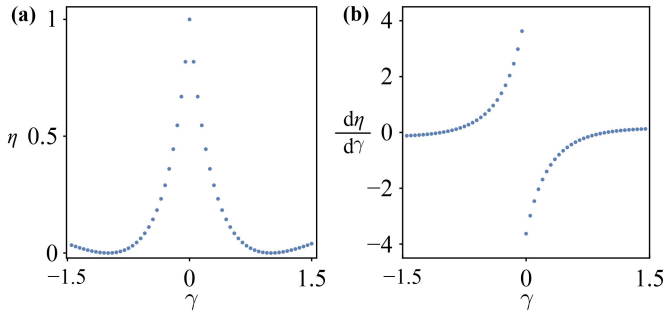

Fig. 2 **(a)** and **(b)** respectively represent the quantity η and its derivative as a function of the parameter γ in the two-level model (3).

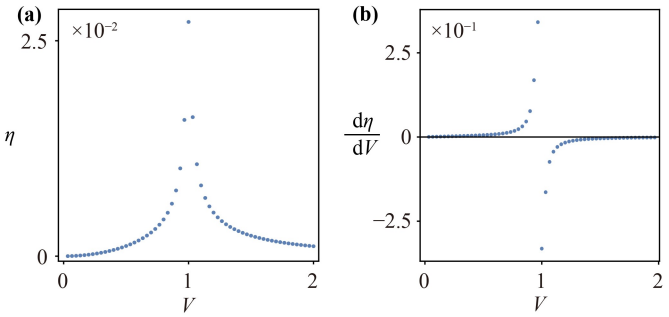

Fig. 3 **(a)** and **(b)** respectively show the quantity η and its derivative as a function of the potential strength V in the model-III (4) [42]. Here, $J_R = 1, J_L = 0.5$.

and the derivative $\frac{\partial\eta}{\partial\delta}|_{\lambda\to 0^{\pm}} = \mp 4$. As shown in Fig. 2, we find that η at EP has a peak and its derivative (denoted as $\partial\eta$) is discontinuous, which is satisfied with our discussion. In the following, we will show that this feature of η can be regarded as an evidence to identify EPs of bulk states in more general non-Hermitian quantum systems.

Since this model-II (3) has merely two levels, the quantity η at EP can take the maximum value 1 and all eigenvectors are coalescent. However, for models with more than two levels, it usually has various EPs with different degeneracies. Consequently, the eigenvectors are not totally coalescent, and the upper bound (denoted as η_c) of η depends on the configuration of EPs: $\eta_c = \frac{\sum_n d_n(d_n-1)}{N(N-1)} \leq 1$, where $N = \sum_n d_n$ is the dimension of Hamiltonian matrix of non-Hermitian systems and n represents nth Jordan block with d_n-fold degeneracy [68]. Only when the non-Hermitian system has one EP with N-degeneracy, the quantity η_c equal to 1 [68].

To illustrate the physics of the discontinuity of $\partial\eta$, we will study two concrete non-Hermitian lattice models. Firstly, we consider a non-Hermitian quasi-crystal lattice model [42] which has a localization-delocalization transition induced by non-Hermiticity:

$$\textbf{Model-III}\quad H = \sum_n (J_R c_{n+1}^{\dagger} c_n + J_L c_n^{\dagger} c_{n+1}) + \sum_n V_n c_n^{\dagger} c_n, \tag{4}$$

where $c_n(c_n^{\dagger})$ is the annihilation (creation) operator of spinless fermion at the nth lattice site. $V_n = V\exp(-2\pi i\alpha n)$ is a site-dependent incommensurate complex potential parameterized by an irrational number α. The potential strength V is positive and real. We set the parameter $\alpha = \sqrt{2} \approx \frac{239}{169}$ same as Ref. [42]. In the practical simulations, we set the length $L = 169$ of the system with periodic boundary condition. As discussed in Ref. [42], metal-insulator phase transition (MIT) of this model-III (4) occurs at the point $V = 1$. In Fig. 3, we can see that the quantity η as a function of V exhibits a sharp peak at $V = 1$, and a discontinuity point of the derivative of η coincides with $V = 1$ point. These features of η in the model-III (4) are similar with the features in the two-level model (3). Therefore, we infer that the model-III (4) contains EPs of bulk states at the MIT transition point, where the EPs are called bulk EPs.

Furthermore, we study a $\mathcal{PT}$-symmetrical SSH model [38] with EPs in bulk states to show the behaviors of the quantity η, where the model is written in momentum space as

$$\textbf{Model-IV}\quad H(k) = \begin{pmatrix} iu & we^{-ik} + v \\ we^{ik} + v & -iu \end{pmatrix}, \tag{5}$$

where the parameters $u, w, v \in \mathbb{R}$, and k is the wave vector (or momentum). $\mathcal{PT}$ symmetry is represented as $\sigma_x H(k)\sigma_x = H^*(k)$. The energy dispersion of the model (5) is $E(k) = \pm\sqrt{|we^{-ik} + v|^2 - u^2}$. Due to absence of skin effect [7], we can use the eigenstates of the Hamiltonian

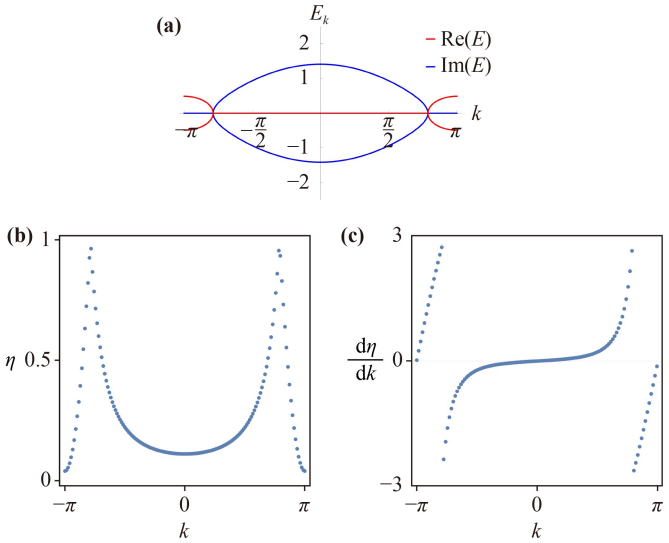

Fig. 4 **(a)** is the energy spectrum of the Hamiltonian (5), **(b)** and **(c)** are respectively the quantity η and its derivative with the wave vector k varying. Here $(w, u, v) = (0.7, 0.5, 0.8)$.

(5) to faithfully represent the bulk states of $\mathcal{PT}$-symmetrical SSH model with open boundary condition. Meanwhile, as discussed in Ref. [38], with $u, w, v > 0$, the $\mathcal{PT}$-broken phase ($|w - v| < u$) of the model-IV (5) has complex energy spectrum and two bulk EPs at $k = \pm \arccos \frac{u^2 - v^2 - w^2}{2vw}$ in Fig. 4(a). Next, without loss of generality, we choose a typical point $(w, u, v) = (0.7, 0.5, 0.8)$ in the $\mathcal{PT}$-broken phase to demonstrate η and its derivative $\frac{\mathrm{d}\eta}{\mathrm{d}k}$ with the wave vector k varying. As shown in Figs. 4(b) and (c), we find two discontinuity points of the derivative $\frac{\mathrm{d}\eta}{\mathrm{d}k}$ located at the EPs, which is satisfied with the correspondence between the discontinuity of $\partial\eta$ and EPs of bulk states. In conclusion, based on our numerical results and theoretical analysis, we propose that bulk EPs cause the discontinuity of the derivative of the quantity η, which is entirely different with edge EPs.

4 Concluding remark

To measure non-unitarity of non-Hermitian systems, we have defined a novel variant of Petermann factor η which takes values within the interval $[0, 1]$. As an efficient and powerful indicator of non-unitarity, the discontinuity of the quantity η helps us identify rich physics in non-Hermitian quantum systems.

In the context of the non-Hermitian lattice systems with EPs, the Hamiltonian matrix is classified as a defective matrix due to its lack of a complete basis of eigenvectors. Meanwhile, the numerical algorithm for diagonalizing such matrix is not convergent [69]. Therefore, it is challenging to directly identify the existence of EPs. Our introduced quantity η provides an alternative route to the features of bulk and edge EPs, e.g., by computing the behavior of η in the parameter space and searching discontinuity. In conclusion, we report the introduction of η and show its efficiency and usefulness in characterizing non-Hermitian physics. For more concrete applications and a systematic analytic theory about η (e.g., physics of the derivative of η of all-th orders, and relation to entanglement [39, 42, 70, 71]), we leave them for future work.

Declarations The authors declare that they have no competing interests and there are no conflicts.

Acknowledgements This work was supported by the National Natural Science Foundation of China (NSFC) Grant No. 12074438, the Guangdong Basic and Applied Basic Research Foundation under Grant No. 2020B1515120100, the Open Project of Guangdong Provincial Key Laboratory of Magnetoelectric Physics and Devices under Grant No. 2022B1212010008, and the Fundamental Research Funds for the Central Universities, Sun Yat-sen University (No. 23ptpy05).

Appendix A: The effective bulk Hamiltonian of non-Hermitian SSH model-I (2) with open boundary condition

In this part, we discuss the effective bulk Hamiltonian of non-Hermitian SSH model-I (2) with open boundary condition to study the properties of transition point. Based on Ref. [7], we do a similarity transformation for the Hamiltonian matrix H of the model-I (2) with N unit cells as

$$\overline{H} = S^{-1} H S, \tag{A-1}$$

where S is a diagonal matrix whose diagonal elements are $\{1, 1, r, r, \cdots, r^{N-1}, r^{N-1}\}$. When take $r = \sqrt{(t_2 - g)/(t_2 + g)}$ and set $t_2 = 1, g = 0.1$, $\overline{H}$ becomes the standard SSH model with intracell hopping $t_1 = \bar{t}_1$ and intercell hopping $\bar{t}_2 = \sqrt{(t_2 - g)(t_2 + g)}$. Furthermore, the effective bulk Hamiltonian of the model-I (2) with open boundary condition in k-space is written as

$$\overline{H}(k) = (t_1 + \bar{t}_2 \cos k)\sigma_x + \bar{t}_2 \sin k \sigma_y. \tag{A-2}$$

From this expression, the transition points of the model-I (2) are $t_1 = \sqrt{t_2^2 - g^2}$, which is consistent with our numerical results and the discussion in Ref. [64]. Furthermore, the bulk properties of H is determined by the effective bulk Hamiltonian $\overline{H}$. Therefore, the effective bulk states of H can be constructed by using $|\overline{\psi}_n\rangle = \mathrm{e}^{-\mathrm{i}kn}|\psi(k)\rangle$, where $|\psi(k)\rangle$ is the eigenstate of $\overline{H}(k)$. Specifically, the right and left bulk effective states of Hamiltonian matrix H are represented as $|\psi_n^R\rangle = S|\overline{\psi}_n\rangle = r^{n-1}\mathrm{e}^{-\mathrm{i}kn}|\psi(k)\rangle$ and $\langle\psi_n^L| = \langle\overline{\psi}_n|S^{-1} = \langle\psi(k)|(1/r)^{n-1}\mathrm{e}^{\mathrm{i}kn}$. Then, based on above discussion, when $t_2 = 1, g = 0.1$, we obtain that the inner product of left and right bulk states at transition point equal to $\langle\psi_n^L|\psi_m^R\rangle = \delta_{n,m}$. Due to the completeness of bi-orthogonal relation, we find that the bulk states at the transition point of the model-I (2) do not have EPs.

Appendix B: The analysis for the edge states in the non-Hermitian SSH model-I (2)

In this part, we analytically obtain the edge states of the non-Hermitian SSH model-I (2) with N unit cells to give an explain about the edge state transition. Based on Eq. (2), and we assume the edge states have the form $|\psi_{\mathrm{edge}}\rangle = (\phi_{1,A}, \phi_{1,B}, \ldots, \phi_{n,A}, \phi_{n,B}, \ldots, \phi_{N,A}, \phi_{N,B})$, where $\phi_{n,A(B)}$ represents the wavefunction on the $A(B)$ sublattice in the nth unit cell. Then the eigenequation $H|\psi_{\mathrm{edge}}\rangle = E_{\mathrm{edge}}|\psi_{\mathrm{edge}}\rangle$ can be concretely written as

$$\begin{aligned} &t_1\phi_{n,A} + (t_2 - g)\phi_{n+1,A} = E_{\mathrm{edge}}\phi_{n,B}, n = 1, 2, \ldots, N-1, \\ &(t_2 + g)\phi_{n-1,B} + t_1\phi_{n,B} = E_{\mathrm{edge}}\phi_{n,A}, n = 2, 3, \ldots, N. \end{aligned} \tag{B-1}$$

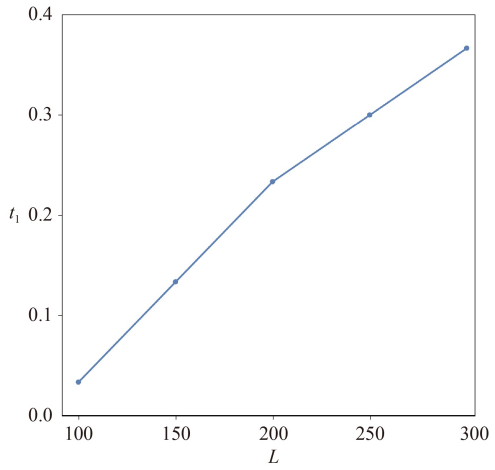

Fig. A1 The location of discontinuity point of η with the size of the model-I increasing. Here $g = 0.1$, $t_2 = 1$.

Furthermore, the boundary conditions are represented as

$$t_1\phi_{1,B} = E_{\text{edge}}\phi_{1,A},$$
$$t_1\phi_{N,A} = E_{\text{edge}}\phi_{N,B}. \tag{B-2}$$

When consider the thermodynamic limit (i.e., $N \to \infty$) and zero-edge states ($E_{\text{edge}} = 0$), we obtain the zero-edge states written as

$$\phi_{n,A} = \left(-\frac{t_1}{t_2 - g}\right)^{n-1} \phi_{1,A},$$
$$\phi_{1,B} = \left(-\frac{t_1}{t_2 + g}\right)^{n-1} \phi_{n,B}. \tag{B-3}$$

Meanwhile, the boundary conditions become as $\phi_{1,B} = \phi_{N,A} = 0$. Without loss of generality, set $t_2 = 1, g = 0.1$ and $t_1 > 0$, when $t_1 < t_2 - g$, then the wavefunctions $\phi_{n,A}$ and $\phi_{n,B}$ are respectively localized at the left and right endpoints of the 1D chain. Consequently, the two wavefunctions are orthogonal and have no contribution to the quantity η. When $t_1 > t_2 - g$, to satisfy the boundary condition $\phi_{N,A} = 0$, then $\phi_{N,A} = \phi_{1,A} = \phi_{n,A} = 0$. Therefore, in this case, the two edge states merge into one edge states, and simultaneously localized at the right endpoint of the 1D chain. For this reason, the edge states of this case have the contribution to the quantity η. Therefore, with the parameter t_1 increasing from $t_1 < t_2 - g$ to $t_1 > t_2 - g$, the edge states of the model-I (2) have edge state transition, and would cause the appearance of the discontinuity point of η located at $t_1 = t_2 - g$. However, as shown in Fig. 1(b), the discontinuity point does not appear at $t_1 = t_2 - g$, we propose the discrepancy of discontinuity point originates from the finite-size effect. As shown in Fig. A1, when we increase the size of model-I (2), we find that the discontinuity point of η becomes more and more close to $t_1 = t_2 - g$, which is satisfied with our analysis.

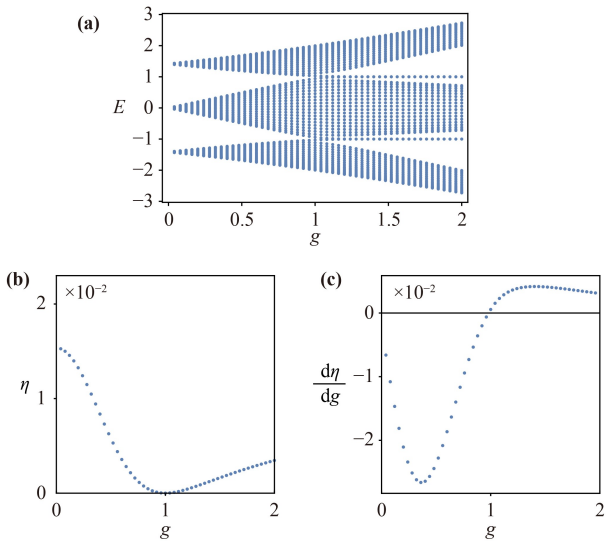

Fig. C1 **(a)** Energy spectrum of the model (C-1) with open boundary condition as a function of the parameter g. **(b)** and **(c)** respectively show the quantity η and its derivative as a function of parameter g.

Appendix C: The behavior of quantity η in a model without EPs

To further investigate the connection between the discontinuity of $\partial\eta$ and the existence of EPs in bulk states, let us consider a 1D non-Hermitian model [72] with topological phase transition at Hermitian point and absence of EPs:

$$\textbf{Model-V}\quad H = t_0 \sum_n \Big(\frac{1}{g} b_n^\dagger a_n + g a_n^\dagger b_n + \frac{1}{g} b_n^\dagger c_n + g c_n^\dagger b_n + g a_{n+1}^\dagger c_n + g c_n^\dagger a_{n+1}\Big), \tag{C-1}$$

where $a_n(a_n^\dagger)$, $b_n(b_n^\dagger)$ and $c_n(c_n^\dagger)$ respectively denote the annihilation(creation) operator of spinless fermions at sublattice A, B and C in the nth unit cell. This model always has real energy spectrum without $\mathcal{PT}$ symmetry. When the parameter $g < 1$ ($g > 1$), the system is trivial (topological) phase. As discussed in Ref. [72], the system with non-trivial Zak phase in the parameter range $g > 1$ has topological edge states as shown in Fig. C1(a).

Keeping the critical point $g = 1$ in mind, we study the value and derivative of η as the functions of the "non-Hermiticity inducer" g in the model-V (C-1) as shown in Figs. C1(b) and (c). We find that η reaches its minimum exactly at $g = 1$ where the derivative vanishes and the model recovers Hermiticity. Apparently, the derivative of η is always continuous in this model, which is different from that in the models-III, IV (4). By careful analysis, we find this difference originates from the model construction [72] of using the regular Sturm-Liouville theory [73] (more discussion see Appendix D). This

theory guarantees the complete basis of the model-V (C-1), so EP is absent in this system. Therefore, without EP, the quantity η and its defective in this model-V (C-1) would not have discontinuity point.

Appendix D: The property of a class of special models and Sturm–Liouville theory

In this part, we discuss the properties of the model-V (C-1). This model is constructed from the equation given as:

$$H_0\Psi_n = E_n M\Psi_n, \tag{D-1}$$

where H_0 is a Hermitian matrix, M is a real diagonal matrix with diagonal element $M_{ii} > 0$. This equation is discussed in the regular Sturm–Liouville theory [73]. Meanwhile, as discussed in Ref. [72], the Hamiltonian matrix of the model-V (C-1) is represented as $M^{-1}H_0$ and non-Hermitian.

Let us review some properties of Eq. (D-1) to demonstrate the model in Ref. [72] having real energy spectrum. Due to the property of the regular Sturm–Liouville theory [73], 0 is not the eigenvalue of H_0. Then, Eq. (D-1) can transformed to

$$\lambda_n M^{\frac{1}{2}}\Psi_n = (M^{\frac{1}{2}}KM^{\frac{1}{2}})M^{\frac{1}{2}}\Psi_n, \tag{D-2}$$

where K is the inverse of H_0, and $\lambda_n = E_n^{-1}$. Furthermore, the matrix $K' = M^{\frac{1}{2}}KM^{\frac{1}{2}}$ is Hermitian, which is proven by

$$(M^{\frac{1}{2}}KM^{\frac{1}{2}})^\dagger = (M^{\frac{1}{2}})^\dagger K^\dagger (M^{\frac{1}{2}})^\dagger = M^{\frac{1}{2}}KM^{\frac{1}{2}}. \tag{D-3}$$

This proof is based on the Hermiticity of the matrices K and $M^{\frac{1}{2}}$. Therefore, from Eq. (D-2), we find the eigenvalues λ_n are real, and the eigenvalues E_n of $M^{-1}H_0$ are real. Meanwhile, we find the eigenvectors $\Psi'_n = M^{\frac{1}{2}}\Psi_n$ are a set of orthogonal and complete basis satisfying the relation:

$$\langle\Psi'_n|\Psi'_m\rangle = \langle\Psi_n|M|\Psi_m\rangle = \delta_{n,m}, \tag{D-4}$$

where $\delta_{n,m}$ is the Kronecker delta. Based on the relation (D-4), the eigenvectors Ψ_n of the matrix $M^{-1}H_0$ are always complete. For a non-Hermitian system with EPs, the basis of eigenvectors is not complete. Then, EP is absent in the model-V (C-1).

References

1. C. M. Bender, Making sense of non-Hermitian Hamiltonians, *Rep. Prog. Phys.* 70(6), 947 (2007)
2. H. Cao and J. Wiersig, Dielectric microcavities: Model systems for wave chaos and non-Hermitian physics, *Rev. Mod. Phys.* 87(1), 61 (2015)
3. I. Rotter, A non-Hermitian Hamilton operator and the physics of open quantum systems, *J. Phys. A Math. Theor.* 42(15), 153001 (2009)
4. Y. Ashida, Z. Gong, and M. Ueda, Non-Hermitian physics, *Adv. Phys.* 69(3), 249 (2020)
5. E. J. Bergholtz, J. C. Budich, and F. K. Kunst, Exceptional topology of non-Hermitian systems, *Rev. Mod. Phys.* 93(1), 015005 (2021)
6. R. Lin, T. Tai, L. Li, and C. H. Lee, Topological non-Hermitian skin effect, *Front. Phys.* 18(5), 53605 (2023)
7. S. Yao and Z. Wang, Edge states and topological invariants of non-Hermitian systems, *Phys. Rev. Lett.* 121(8), 086803 (2018)
8. K. Yokomizo and S. Murakami, Non-Bloch band theory of non-Hermitian systems, *Phys. Rev. Lett.* 123(6), 066404 (2019)
9. Z. Yang, K. Zhang, C. Fang, and J. Hu, Non-Hermitian bulk–boundary correspondence and auxiliary generalized Brillouin zone theory, *Phys. Rev. Lett.* 125(22), 226402 (2020)
10. W. D. Heiss, The physics of exceptional points, *J. Phys. A* 45(44), 444016 (2012)
11. T. Gao, E. Estrecho, K. Y. Bliokh, T. C. H. Liew, M. D. Fraser, S. Brodbeck, M. Kamp, C. Schneider, S. Höfling, Y. Yamamoto, F. Nori, Y. S. Kivshar, A. G. Truscott, R. G. Dall, and E. A. Ostrovskaya, Observation of non-Hermitian degeneracies in a chaotic exciton–polariton billiard, *Nature* 526(7574), 554 (2015)
12. B. Zhen, C. W. Hsu, Y. Igarashi, L. Lu, I. Kaminer, A. Pick, S. L. Chua, J. D. Joannopoulos, and M. Soljačić, Spawning rings of exceptional points out of Dirac cones, *Nature* 525(7569), 354 (2015)
13. C. Hahn, Y. Choi, J. W. Yoon, S. H. Song, C. H. Oh, and P. Berini, Observation of exceptional points in reconfigurable non-Hermitian vector-field holographic lattices, *Nat. Commun.* 7(1), 12201 (2016)
14. D. Zhang, X. Q. Luo, Y. P. Wang, T. F. Li, and J. Q. You, Observation of the exceptional point in cavity magnon-polaritons, *Nat. Commun.* 8(1), 1368 (2017)
15. M. A. Miri and A. Alù, Exceptional points in optics and photonics, *Science* 363(6422), eaar7709 (2019)
16. S. Wang, B. Hou, W. Lu, Y. Chen, Z. Q. Zhang, and C. T. Chan, Arbitrary order exceptional point induced by photonic spin–orbit interaction in coupled resonators, *Nat. Commun.* 10(1), 832 (2019)
17. L. Xiao, T. Deng, K. Wang, Z. Wang, W. Yi, and P. Xue, Observation of non-Bloch parity–time symmetry and exceptional points, *Phys. Rev. Lett.* 126(23), 230402 (2021)
18. H. Hu, S. Sun, and S. Chen, Knot topology of exceptional point and non-Hermitian no–go theorem, *Phys. Rev. Res.* 4(2), L022064 (2022)
19. F. K. Kunst, E. Edvardsson, J. C. Budich, and E. J. Bergholtz, Biorthogonal bulk–boundary correspondence in non-Hermitian systems, *Phys. Rev. Lett.* 121(2), 026808 (2018)
20. C. H. Lee and R. Thomale, Anatomy of skin modes and topology in non-Hermitian systems, *Phys. Rev. B* 99(20), 201103 (2019)
21. N. Okuma, K. Kawabata, K. Shiozaki, and M. Sato, Topological origin of non-Hermitian skin effects, *Phys. Rev. Lett.* 124(8), 086801 (2020)

22. N. Okuma and M. Sato, Non-Hermitian skin effects in Hermitian correlated or disordered systems: Quantities sensitive or insensitive to boundary effects and pseudo-quantum-number, *Phys. Rev. Lett.* 126(17), 176601 (2021)
23. K. Zhang, Z. Yang, and C. Fang, Universal non-Hermitian skin effect in two and higher dimensions, *Nat. Commun.* 13(1), 2496 (2022)
24. Z. Lin, H. Ramezani, T. Eichelkraut, T. Kottos, H. Cao, and D. N. Christodoulides, Unidirectional invisibility induced by *PT*-symmetric periodic structures, *Phys. Rev. Lett.* 106(21), 213901 (2011)
25. S. Yao, F. Song, and Z. Wang, Non-Hermitian Chern bands, *Phys. Rev. Lett.* 121(13), 136802 (2018)
26. T. S. Deng and W. Yi, Non-Bloch topological invariants in a non-Hermitian domain wall system, *Phys. Rev. B* 100(3), 035102 (2019)
27. T. Liu, Y. R. Zhang, Q. Ai, Z. Gong, K. Kawabata, M. Ueda, and F. Nori, Second-order topological phases in non-Hermitian systems, *Phys. Rev. Lett.* 122(7), 076801 (2019)
28. S. Longhi, Non-Bloch-band collapse and chiral Zener tunneling, *Phys. Rev. Lett.* 124(6), 066602 (2020)
29. K. Zhang, Z. Yang, and C. Fang, Correspondence between winding numbers and skin modes in non-Hermitian systems, *Phys. Rev. Lett.* 125(12), 126402 (2020)
30. K. Kawabata, N. Okuma, and M. Sato, Non-Bloch band theory of non-Hermitian Hamiltonians in the symplectic class, *Phys. Rev. B* 101(19), 195147 (2020)
31. H. Shen, B. Zhen, and L. Fu, Topological band theory for non-Hermitian Hamiltonians, *Phys. Rev. Lett.* 120(14), 146402 (2018)
32. Z. Gong, Y. Ashida, K. Kawabata, K. Takasan, S. Higashikawa, and M. Ueda, Topological phases of non-Hermitian systems, *Phys. Rev. X* 8(3), 031079 (2018)
33. K. Kawabata, T. Bessho, and M. Sato, Classification of exceptional points and non-Hermitian topological semimetals, *Phys. Rev. Lett.* 123(6), 066405 (2019)
34. K. Kawabata, K. Shiozaki, M. Ueda, and M. Sato, Symmetry and topology in non-Hermitian physics, *Phys. Rev. X* 9(4), 041015 (2019)
35. H. Zhou and J. Y. Lee, Periodic table for topological bands with non-Hermitian symmetries, *Phys. Rev. B* 99(23), 235112 (2019)
36. L. Herviou, N. Regnault, and J. H. Bardarson, Entanglement spectrum and symmetries in non-Hermitian fermionic non-interacting models, *SciPost Phys.* 7, 069 (2019)
37. C. C. Wojcik, X. Q. Sun, T. Bzdušek, and S. Fan, Homotopy characterization of non-Hermitian Hamiltonians, *Phys. Rev. B* 101(20), 205417 (2020)
38. P. Y. Chang, J. S. You, X. Wen, and S. Ryu, Entanglement spectrum and entropy in topological non-Hermitian systems and nonunitary conformal field theory, *Phys. Rev. Res.* 2(3), 033069 (2020)
39. L. M Chen, S. A. Chen, and P. Ye, Entanglement, non-hermiticity, and duality, *SciPost Phys.* 11, 003 (2021)
40. S. Sayyad, J. Yu, A. G. Grushin, and L. M. Sieberer, Entanglement spectrum crossings reveal non-Hermitian dynamical topology, *Phys. Rev. Res.* 3(3), 033022 (2021)
41. Y. B. Guo, Y. C. Yu, R. Z. Huang, L. P. Yang, R. Z. Chi, H. J. Liao, and T. Xiang, Entanglement entropy of non-Hermitian free fermions, *J. Phys.: Condens. Matter* 33(47), 475502 (2021)
42. L. M. Chen, Y. Zhou, S. A. Chen, and P. Ye, Quantum entanglement of non-Hermitian quasicrystals, *Phys. Rev. B* 105(12), L121115 (2022)
43. S. Longhi, Topological phase transition in non-Hermitian quasicrystals, *Phys. Rev. Lett.* 122(23), 237601 (2019)
44. Q. B. Zeng and Y. Xu, Winding numbers and generalized mobility edges in non-Hermitian systems, *Phys. Rev. Res.* 2(3), 033052 (2020)
45. Y. Liu, X. P. Jiang, J. Cao, and S. Chen, Non-Hermitian mobility edges in one-dimensional quasicrystals with parity–time symmetry, *Phys. Rev. B* 101(17), 174205 (2020)
46. Y. Liu, Q. Zhou, and S. Chen, Localization transition, spectrum structure, and winding numbers for one-dimensional non-Hermitian quasicrystals, *Phys. Rev. B* 104(2), 024201 (2021)
47. N. Hatano and D. R. Nelson, Localization transitions in Non-Hermitian quantum mechanics, *Phys. Rev. Lett.* 77(3), 570 (1996)
48. N. Hatano and D. R. Nelson, Vortex pinning and non-Hermitian quantum mechanics, *Phys. Rev. B* 56(14), 8651 (1997)
49. N. Hatano and D. R. Nelson, Non-Hermitian delocalization and eigenfunctions, *Phys. Rev. B* 58(13), 8384 (1998)
50. Q. Lin, T. Li, L. Xiao, K. Wang, W. Yi, and P. Xue, Observation of non-Hermitian topological Anderson insulator in quantum dynamics, *Nat. Commun.* 13(1), 3229 (2022)
51. C. M. Bender, Introduction to $\mathcal{PT}$-symmetric quantum theory, *Contemp. Phys.* 46(4), 277 (2005)
52. J. Wiersig, Nonorthogonality constraints in open quantum and wave systems, *Phys. Rev. Res.* 1(3), 033182 (2019)
53. K. Petermann, Calculated spontaneous emission factor for double-heterostructure injection lasers with gain-induced waveguiding, *IEEE J. Quantum Electron.* 15(7), 566 (1979)
54. K. G. Makris, R. El-Ganainy, D. N. Christodoulides, and Z. H. Musslimani, Beam dynamics in *PT* symmetric optical lattices, *Phys. Rev. Lett.* 100(10), 103904 (2008)
55. H. Schomerus, Excess quantum noise due to mode nonorthogonality in dielectric microresonators, *Phys. Rev. A* 79(6), 061801 (2009)
56. J. Wiersig, A. Eberspächer, J. B. Shim, J. W. Ryu, S. Shinohara, M. Hentschel, and H. Schomerus, Nonorthogonal pairs of copropagating optical modes in deformed microdisk cavities, *Phys. Rev. A* 84(2), 023845 (2011)
57. Y. V. Fyodorov and D. V. Savin, 0, Statistics of resonance width shifts as a signature of eigenfunction nonorthogonality, *Phys. Rev. Lett.* 108(18), 184101 (2012)
58. K. G. Makris, L. Ge, and H. E. Türeci, Anomalous transient amplification of waves in non-normal photonic media, *Phys. Rev. X* 4(4), 041044 (2014)
59. M. Davy and A. Z. Genack, Selectively exciting quasi-normal modes in open disordered systems, *Nat. Commun.* 9(1), 4714 (2018)

60. M. Davy and A. Z. Genack, Probing nonorthogonality of eigenfunctions and its impact on transport through open systems, *Phys. Rev. Res.* 1(3), 033026 (2019)
61. F. Song, S. Yao, and Z. Wang, Non-Hermitian topological invariants in real space, *Phys. Rev. Lett.* 123(24), 246801 (2019)
62. T. D. Lee and L. Wolfenstein, Analysis of *CP*-noninvariant interactions and the $k_1{}^0$, $k_2{}^0$ system, *Phys. Rev.* 138(6B), B1490 (1965)
63. H. Wang, Y. H. Lai, Z. Yuan, M. G. Suh, and K. Vahala, Petermann-factor sensitivity limit near an exceptional point in a Brillouin ring laser gyroscope, *Nat. Commun.* 11(1), 1610 (2020)
64. J. Cheng, X. Zhang, M. H. Lu, and Y. F. Chen, Competition between band topology and non-Hermiticity, *Phys. Rev. B* 105(9), 094103 (2022)
65. Z. Oztas and N. Candemir, Su–Schrieffer–Heeger model with imaginary gauge field, *Phys. Lett. A* 383(15), 1821 (2019)
66. X. R. Wang, C. X. Guo, and S. P. Kou, Defective edge states and number-anomalous bulk–boundary correspondence in non-Hermitian topological systems, *Phys. Rev. B* 101(12), 121116 (2020)
67. W. Zhu, W. X. Teo, L. Li, and J. Gong, Delocalization of topological edge states, *Phys. Rev. B* 103(19), 195414 (2021)
68. Y. Zhou, L. M. Chen, and P. Ye, to be appeared (2023)
69. J. W. Demmel, Nearest defective matrices and the geometry of ill-conditioning, *Reliable Numer. Comput.* 44, 35 (1990)
70. C. H. Lee, P. Ye, and X. L. Qi, Position–momentum duality in the entanglement spectrum of free fermions, *J. Stat. Mech.* 2014(10), P10023 (2014)
71. C. H. Lee and P. Ye, Free-fermion entanglement spectrum through Wannier interpolation, *Phys. Rev. B* 91(8), 085119 (2015)
72. Y. Long, H. Xue, and B. Zhang, Non-Hermitian topological systems with eigenvalues that are always real, *Phys. Rev. B* 105(10), L100102 (2022)
73. A. Zettl, Sturm–Liouville Theory, 121, American Mathematical Society, 2012